

Mechanic-Electric Coupling Characteristics of a Resonant Tunneling Diode*

Tong Zhaomin[†], Xue Chenyang, Lin Yijie, and Chen Shang

(National Key Laboratory of Electronic Measurement Technology, Key Laboratory of Instrumentation Science & Dynamic Measurement, Ministry of Education, North University of China, Taiyuan 030051, China)

Abstract: This paper reports the piezoresistive effect of a resonant tunneling diode (RTD) in a microstructure. The four-beam structure is analyzed and fabricated by positing RTDs at the stress sensitive regions. Stress along the $[110]$ orientation and $[1\bar{1}0]$ orientation induces a change in the RTD's current-voltage (I - V) curves, i. e., the meso-piezoresistance variety, mainly in its negative differential resistance (NDR) region. By different methods, the mechanic-electric coupling characteristic of RTD is studied and the consistent 10^{-9} Pa^{-1} piezoresistive coefficients are discovered.

Key words: piezoresistive effect; RTD; NDR; mechanic-electric coupling

PACC: 7360L; 8170

CLC number: TN304.93

Document code: A

Article ID: 0253-4177(2008)10-1907-06

1 Introduction

The advantages of MEMS over conventional fabrication, such as improved dimensional control, extreme miniaturization, the ability to integrate with on-chip circuitry, and potential low-cost as a result of batch processing, have attracted attention in recent decades. Compared with silicon (Si), gallium arsenide (GaAs) has many merits, such as a nonzero piezoelectric coefficient, a higher Peltier coefficient, direct band gap facilitating efficient two-way conversion between electrical energy and light, higher radiation hardness, lower stiffness, and wider operative temperature range^[1]. The piezoelectric $\text{Al}_{0.3}\text{Ga}_{0.7}\text{As}$ microstructure has been used on MEMS fabrication^[2], and by the piezoresistive effect of GaAs, pressure sensors have been fabricated with GaAs/AlGaAs membrane technology, the responsivity of which is nearly constant up to temperatures of 433K^[3].

Recently, with the rapid development of molecular beam epitaxy (MBE), metal organic chemical vapor deposition (MOCVD), and the technology of etch methods, many kinds of quantum well materials can be grown and fabricated^[4]. RTD is such a quantum well material with the NDR effect in the I - V characteristics and has attracted elevated attention due to electronic and photonic applications. The remarkably fast-acting NDR region behavior (i. e., an initial rise of the current followed by a sharp decrease when the voltage is progressively increased) makes it an excellent device for very high-frequency electronic applications and more complex memory and logic cir-

uits^[5,6]. These resonant tunneling structures may be used as an oscillator with operating frequency as high as 712GHz and a mixer with an operating frequency of 2.5THz^[7]. The latter is concentrated on using the unique electronic and optic properties of these devices for lasers, detectors, and modulators in the infrared to visible wavelength range, and high-speed optically switched electronic devices. However, the RTD I - V characteristics show special uniaxial stress dependence, mainly in the NDR region. This dependence has been applied to mechanic-electric exchange and used to design new sensors, such as pressure sensors^[8,9].

In this paper, GaAs/AlAs/InGaAs resonant tunneling structures are grown by MBE on $[001]$ semi-insulating GaAs substrate and a four-beam structure with RTDs posited at its sensitive regions is processed successfully by control-hole technology. I - V curves of RTD under different applied pressures show -1.51×10^{-9} and $3.03 \times 10^{-9} \text{ Pa}^{-1}$ piezoresistive coefficients in the NDR region along the $[110]$ orientation and $[1\bar{1}0]$ orientation, respectively. We also apply a centrifugal machine to detect this mechanic-electric coupling characteristic in the microstructure, and furthermore, by a Wheatstone circuit, this phenomenon is confirmed on a jarring table. The 10^{-9} Pa^{-1} piezoresistive coefficients are consistent with each other.

2 Design and fabrication

2.1 Structure design

The model of the four-beam structure is shown in

* Project supported by the National Natural Science Foundation of China (Nos. 50535030, 50775209) and the Program for New Century Excellent Talents in University

[†] Corresponding author. Email: tong-zhaomin@sohu.com

Received 12 January 2008, revised manuscript received 18 June 2008

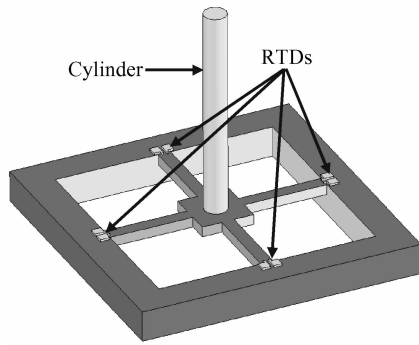


Fig.1 Model of the structure with RTDs at the root of beams

Fig.1. It consists of a block supported by four beams and RTDs posited at the root of each beam to obtain the largest stress. The cylinder, for transferring $[110]$ orientation and $[\bar{1}\bar{1}0]$ orientation force, is fixed at the central block.

According to Xue *et al.*^[10], the stress $\sigma(x)$ in the beam at location x undergoing the action of $M(x)$ can be expressed by

$$\sigma(x) = \frac{L^2 + 3aL - 3x(a + L)}{\frac{2}{3}bt^2(L^2 + 3aL + 3a^2)} mg \frac{h}{2} \quad (1)$$

where L , b , and t are the beam's length, width, and depth, respectively, a is the length of central block's side, and m , h are the mass and height of the cylinder.

2.2 Fabrication

The resonant tunneling structures are grown by MBE on $[001]$ orientation semi-insulated GaAs substrate, as shown in Table 1. On the substrate is a $1\mu\text{m}$ heavily doped n-type ($3 \times 10^{18} \text{ cm}^{-3}$) GaAs collector Ohmic contact layer, followed by a 10nm heavily doped n-type (10^{17} cm^{-3}) GaAs collector layer; the

Table 1 GaAs/AlAs/InGaAs resonant tunneling structures grown by MBE

Depth/nm	Material	Concentration/ cm^{-3}
500	n^+ -GaAs	3×10^{18}
10	n^+ -GaAs	10^{17}
5	GaAs	Undoped (UD)
5	$\text{In}_{0.1}\text{Ga}_{0.9}\text{As}$	UD
0.5	GaAs	UD
1.7	AlAs	UD
0.5	GaAs	UD
4	$\text{In}_{0.1}\text{Ga}_{0.9}\text{As}$	UD
0.5	GaAs	UD
1.7	AlAs	UD
0.5	GaAs	UD
5	$\text{In}_{0.1}\text{Ga}_{0.9}\text{As}$	UD
5	GaAs	UD
10	n^+ -GaAs	10^{17}
1000	n^+ -GaAs	3×10^{18}
75mm n^+ /SI-GaAs substrate		

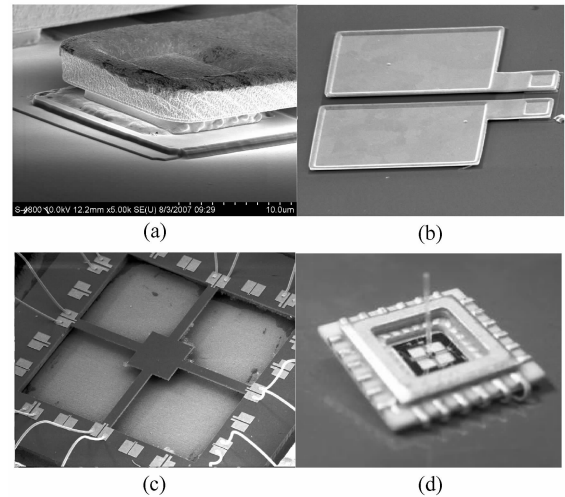


Fig.2 Illustration of the progress steps (a) SEM of the resonant tunneling structures and AuGe/Ni/Au Ohmic contact; (b) SEM of RTD; (c) SEM of the structure with a central block supported by four beams; (d) Package map of the structure with a cylinder fixed on the central block

GaAs/AlAs/InGaAs resonant tunneling structures are grown with two undoped GaAs/InGaAs/GaAs interlayers to prevent the diffusion of collector and emitter doped layers, and the double barrier single well GaAs/AlAs/InGaAs sandwich structures are chucked in the center; finally, the 10nm heavily doped n-type (10^{17} cm^{-3}) GaAs emitter layer is grown, with a 500nm heavily doped n-type ($3 \times 10^{18} \text{ cm}^{-3}$) GaAs emitter ohmic contact layer above it.

We begin the fabrication of RTD with the $8\mu\text{m} \times 8\mu\text{m}$ square emitter mesa etched by reactive ion etching (RIE), followed by AuGe/Ni/Au Ohmic contact deposition, patterning, and annealing at 420°C for 10 seconds, as shown in Fig. 2 (a). After collector mesa photolithography and Si_3N_4 deposition, the electrodes are formed by an air-bridge structure to provide measurements under applied bias, shown in Fig. 2 (b). The four-beam structure is processed by control-hole technology. First, the $10\mu\text{m}$ deep hole and the structure are etched by ICP in the front side, then the back side etching stopped when the hole is visible, and the remains, namely the required structure, is released, as shown in Fig. 2 (c). Finally, the sensor is packaged with a cylinder fixed on the central block, as shown in Fig. 2 (d).

3 Measurements and discussion

3.1 Raman spectroscopy system

The stress change can be calculated by Raman spectroscopy accurately and with no destructivity. When the sample is pressured, the energy of vibration

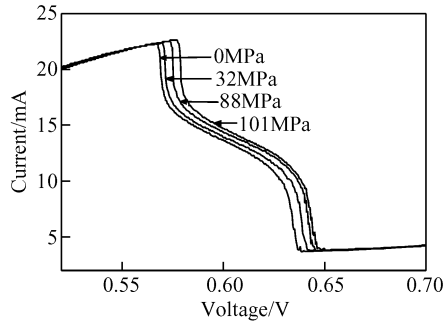


Fig. 3 *I-V* curves of RTD under applied stress along the $[110]$ orientation^[12]

changes and the Raman band is shifted to higher (compression) or lower (expansion) energy. For $[001]$ orientation GaAs, the Raman shifts with stress have the following relationship^[11]:

$$\sigma_{xx} = -576\Delta\omega \quad (2)$$

where σ_{xx} is the stress, $\Delta\omega$ is the Raman shift, and “-” means that the stress is a tensile stress.

Figures 3 and 4 show the *I-V* curves of RTD with pressure variety measured by a RENISHAW inVia Raman spectroscope and an Agilent4156C semiconductor analyzer. The pressure is brought by a probing station along the $[110]$ orientation and $[1\bar{1}0]$ orientation^[12]. Because of different batches of device fabrication, the biased voltage of their NDR regions varies slightly.

Assuming the biased voltage of RTD is a constant value and that the current’s variety induced can be replaced by the change of relative resistance, the meso-piezoresistive coefficient is defined as

$$S = \frac{\Delta R}{R\sigma} = \frac{R_i - R_0}{R_0\sigma} \quad (3)$$

where $\Delta R/R$ is the relative change of resistance, and σ is the stress measured by the Raman spectroscope. The linear meso-piezoresistive coefficient of RTD is calculated to be -1.51×10^{-9} and $3.03 \times 10^{-9} \text{ Pa}^{-1}$ in the NDR region along the $[110]$ and $[1\bar{1}0]$ orientation, respectively, as shown in Fig. 5.

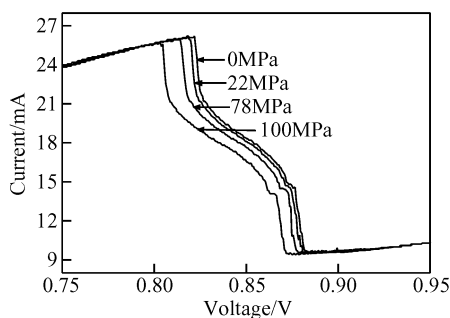


Fig. 4 *I-V* curves of RTD under applied stress along the $[1\bar{1}0]$ orientation^[12]

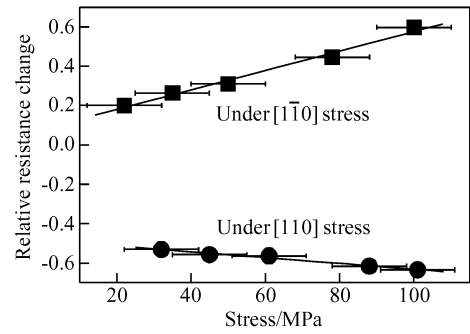


Fig. 5 Largest piezoresistive coefficients along the $[110]$ and $[1\bar{1}0]$ orientation^[12]

3.2 Coupling in structure

Two methods, *I-V* curves calculation and the Wheatstone circuit solution, have been introduced. The former is tested on a centrifugal machine, with the cylinder vertical to horizontal and the beams perpendicular and/or vertical to the centrifugal radial axle. *I-V* curves of the RTD are measured by an Agilent4156C semiconductor analyzer. To deduce or eliminate the air damp when the cylinder is running, a rubber cap covering the packaged structure has been used. Because of centrifugal force, the cylinder will bend and induce stress in the beams. By Eq. (1), the stress change under different centrifugal acceleration in the beams’ roots can be calculated, and by Eq. (3), varieties of the largest relative resistance are obtained, as shown in Fig. 6.

The latter is tested on a jarring table, with the cylinder perpendicular to horizontal. Like measurement on centrifugal machine, a rubber cap is also introduced. An important characteristic of RTD is its high frequency relaxation oscillation when biased in the NDR region^[13]. For the piezoresistive measurement, this oscillation frequency should be avoided or eliminated. A Max291 low-pass filter is introduced and the circuit output noise can be reduced to 20 ~ 30mV (after the amplifier, the amplification ratio is

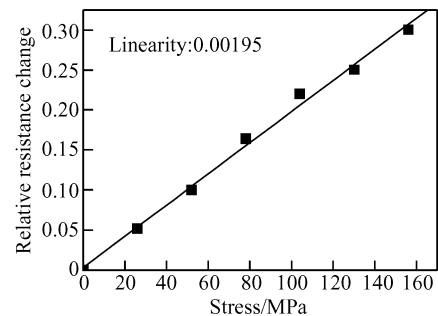


Fig. 6 Largest piezoresistive coefficient measured on centrifugal machine

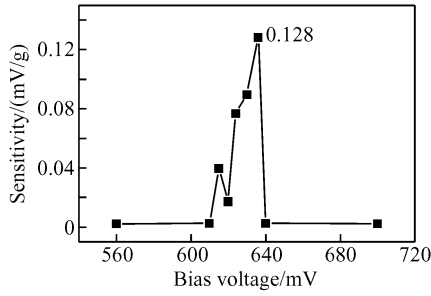


Fig. 7 Output voltage by Wheatstone circuit biased at different voltages of RTD^[10]

4680). Testing has been conducted by a Wheatstone bridge circuit, which consists of two little value resistors (1Ω), an adjustable resistor, and RTD. At 0.5g acceleration, the output voltages with different biased voltage of RTD are obtained, as shown in Fig. 7. Because the resistors, capacitors, *et al.* are in series and/or parallel with the RTD, the NDR region becomes narrow^[14].

Assuming the resistances of RTD and the adjustable resistor are R_x and R_1 , the resistances of the two little value resistors are R_2 , the input voltage is V_{in} , the amplification ratio of the circuit is G , and the output voltage is V_{out} , we obtain the following equation.

$$V_{out} = \left(\frac{R_x}{R_1 + R_x} V_{in} - \frac{R_2}{R_1 + R_2} V_{in} \right) G \quad (4)$$

Adjusting R_1 implies that when $R_1 = R_x$, the circuit will be balanceable. Assuming the change of RTD under stress is ΔR_x , which is much less than R_x , then Equation (4) can be expressed as

$$V_{out} = \frac{\Delta R_x}{2R_x} G V_{in} \quad (5)$$

From Eq. (5), the output voltage has a direct relationship with relative resistance change. In Fig. 7, we have illustrated the output voltage with different biased voltages of RTD. The figure shows that in the valley voltage region (0.636mV approximately), the output voltage reaches its maximum value, about 0.3V. The induced stress can be calculated by Eq. (1), and thus the piezoresistive coefficient, $1.78 \times 10^{-9} \text{ Pa}^{-1}$, is obtained. Table 2 displays the largest piezoresistive coefficients calculated by different methods, and the results match well with each other.

Table 2 Largest piezoresistive coefficients calculated by different methods

Method	Piezoresistive coefficients along orientation/ 10^{-9} Pa^{-1}	
	[110]	[1 $\bar{1}$ 0]
Raman spectroscopy	-1.51	3.03
Centrifugal machine	1.95	
Jarring table	1.78	

3.3 Discussion

According to Wen^[15], the external strain in super-lattices results from the mechanical interaction between two adjacent layers. At room temperature and normal pressure, if the interference is zero, the tetragonal distortion can be written as

$$\Delta \epsilon' = \Delta \tilde{\epsilon} [\beta - \beta^{\lambda}] \Delta T_g \quad (6)$$

where ΔT_g is the difference between growth temperature and room temperature, β is the thermal expansion coefficient at the room temperature, β^{λ} is the in-plane linear thermal expansion coefficient, and $\Delta \tilde{\epsilon}$ is determined by the elastic constant and growth direction of the super-lattices. In general cases, the external strain can be written as

$$\Delta \epsilon = \Delta \epsilon^{\lambda} + \delta \epsilon \quad (7)$$

where $\delta \epsilon$ depends on the growth interference and can be calculated and measured quantitatively.

Because of the difference in piezoelectric constants between the AlAs and GaAs layers^[16], when subjected to stress fields, the polarization charges will be induced at the interfaces in each layer and will generate piezoelectric fields in the barriers and the well of the resonant tunneling structures. A general description of the built-in electric field and strain can be described as

$$E = A \Delta \epsilon \quad (8)$$

where A is a constant. The built-in electric fields will result in the formation of valence band offset difference ΔV_B on the two sides of a barrier, which can be defined as

$$\Delta V_B = e \begin{cases} \sum_{i=1}^2 \int_{h_0}^{h_i} E_i(x) dx \text{ and } 0, & e'_1 e'_2 > 0 \\ \int_0^{h_1} E_1(x) dx \text{ and } \int_0^{h_2} E_2(x) dx, & e'_1 e'_2 < 0 \\ \int_0^h E(x) dx \text{ and } 0, & e'_1 e'_2 = 0 \end{cases} \quad (9)$$

where e is the electron charge, e'_1 and e'_2 are the piezoelectric coefficients for the two adjacent layers, respectively, and h_i is the thickness of the piezoelectric layer ($i = 1, 2$).

Under [110] stress, the piezoelectric constant of the AlAs layer is larger than that of the GaAs layer^[16] and the direction of the electric field is antiparallel to that of the applied electric field E_a for positive bias. Therefore, higher applied voltage is needed to reach the resonant tunneling condition, as shown in Figs. 8 (a) and 9 (a). However, for [1 $\bar{1}$ 0] stress, the polarization charges oppositely at each heterointerface compared with the [110] case. Hence, more negative applied voltages are needed to obtain resonant tunneling, as shown in Figs. 8 (b) and 9 (b)^[17].

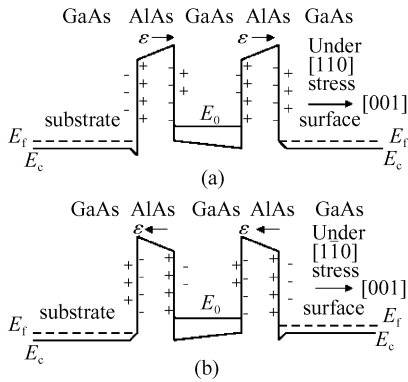


Fig.8 Schematic band diagram and polarization charge distribution for [001] oriented RTD under stress (a) Along the [110] orientation; (b) Along the [1 $\bar{1}$ 0] orientation^[17]

In order to simplify the theoretical expression, the Landauer resistance is defined as

$$R_L = \frac{h}{e^2} \times \frac{R(\Delta V_B)}{T(\Delta V_B)} \quad (10)$$

From Eqs. (6) to (10), R_L can be written as a function of the strain $\Delta\epsilon$:

$$R_L = f(\Delta\epsilon) \quad (11)$$

This is the mathematical expression for the meso-piezoresistive effect, and therefore it can be calculated quantitatively.

4 Conclusion

The mechanical characteristics of the structure, consisting of a central block supported by four beams and a cylinder, are calculated. We have fabricated this structure by control-hole technology, and the RTDs are posited on the root of the beams to obtain the largest stress. The piezoresistive effect of RTD is studied

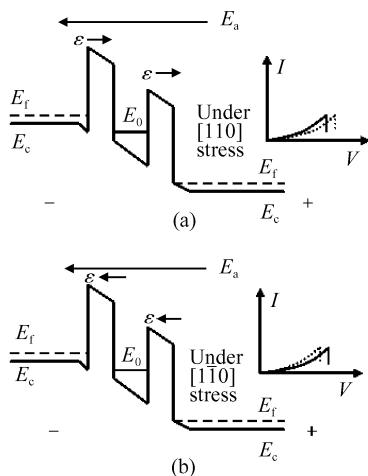


Fig.9 Schematic band diagram and I - V curves for positive bias for [001] oriented RTD under stress (a) Along the [110] orientation; (b) Along the [1 $\bar{1}$ 0] orientation The solid I - V curve represents the current without applied stress and the dotted curve represents the current with applied stress^[17].

both by I - V curve changes and Wheatstone bridge circuits with good consistence. The 10^{-9} order piezoresistive coefficient, along the [110] orientation and the [1 $\bar{1}$ 0] orientation, shows high mechanic-electric coupling characteristics for these resonant tunneling structures.

Further research will focus on the applications of this mechanic-electric coupling characteristic and determining whether this piezoresistive effect can really best that of silicon.

Acknowledgement The authors would like to thank the China Electronics Technology Group Cooperation, 13th Research Institute for help with the RTD's fabrication.

References

- [1] Stark B. MEMS reliability assurance guidelines for space applications. California: JPL Publication, 1999
- [2] Kumara P, Li L, Calhoun L, et al. Fabrication of piezoelectric $Al_{0.3}Ga_{0.7}As$ microstructures. Sensors and Actuators A, 2004, 115:96
- [3] Dehe A, Fricke K, Mutamba K, et al. A piezoresistive GaAs pressure sensor with GaAs/AlGaAs membrane technology. J Micro-mech Microeng, 1995, 5:139
- [4] Kaniewska M, Engström O. Deep traps at GaAs/GaAs interface grown by MBE-interruption growth technique. Mater Sci Eng C, 2007, 27:1069
- [5] Söderström J, Anderson T G. A multiple-state memory cell based on the resonant tunneling diode. IEEE Electron Device Lett, 1988, 9:2163
- [6] Yan Z X, Deen M J. A new resonant-tunneling diode-based multi-valued memory circuit using MESFET depletion load. IEEE J Solid-State Circuits, 1992, 27:1198
- [7] Sollner T C L G, Goodhue W D, Tannenwald P E, et al. Resonant tunneling through quantum wells at frequencies up to 2.5 THz. Appl Phys Lett, 1983, 43(6):588
- [8] Fobelets K, Vounckx R, Borghs G. A GaAs pressure sensor based on resonant tunnelling diodes. J Micromech Microeng, 1994, 4:123
- [9] Mutamba K, Flath M, Sigurdardottir A, et al. A GaAs pressure sensor with frequency output based on resonant tunneling diodes. IEEE Trans Instrum Meas, 1999, 48(6):1333
- [10] Xue Chenyang, Chen Shang, Qiao Hui, et al. Development of a novel two axis piezoresistive micro accelerometer based on silicon. Sensor Letters, 2008, 6(1):149
- [11] Sang Shengbo, Xue Chengyang, Zhang Wendong, et al. Raman quantitate stress in nano-thin film of MEMS. Solid State Phenomena, 2007, 121~123:943
- [12] Liu Wenyi, Tong Zhaomin, Xue Chenyang, et al. Design, fabrication and testing of GaAs/AlAs/InGaAs resonant tunneling vector hydrophones. Sensor Letters, 2008, 6(2):272
- [13] Grubin H L, Buggeln R C. RTD relaxation oscillations and the time-dependent Wigner equation. Phys B: Condensed Matter, 2002, 314(1~4):117
- [14] Sen S, Capasso F, Sivco D, et al. New resonant-tunneling devices with multiple negative resistance regions and high room-temperature peak-to-valley ratio. IEEE Electron Device Lett, 1988, 9(8):402
- [15] Wen T D, Xu L P, Xiong J J, et al. The meso-piezo-resistive effects in MEMS/NEMS. Solid State Phenomena, 2007, 121~123:

- 619
- [16] Mutamba K, Sigurdardottir A, Vogt A, et al. A comparative study of uniaxial pressure effects in intraband AlGaAs/GaAs and intraband InAs/AlSb/GaSb resonant tunneling diodes. Appl Phys Lett, 1998, 72(13):1629
- [17] Cong L, Albrecht J D, Nathan M I, et al. Piezoelectric effects in (001)- and (111)-oriented double barrier resonant tunneling devices. J Appl Phys, 1996, 79:7770

共振隧穿二极管的力电耦合特性*

仝召民[†] 薛晨阳 林沂杰 陈 尚

(中北大学电子测试技术国家重点实验室 中北大学仪器科学与动态测试教育部重点实验室, 太原 030051)

摘要: 报道了微结构中共振隧穿二极管(RTD)的压阻效应. 分析并加工了四梁结构, 其中 RTD 置于应力敏感区. 沿[110]晶向和 $[1\bar{1}0]$ 晶向的应力导致 RTD 电流-电压曲线的改变, 即介观压阻变化, 尤其是在微分负阻(NDR)区. 采用不同测试方法, 研究了 RTD 的力电耦合特性, 并获得了较相近的压阻系数为 10^{-9} Pa^{-1} .

关键词: 压阻效应; RTD; NDR; 力电耦合

PACC: 7360L; 8170

中图分类号: TN304.93

文献标识码: A

文章编号: 0253-4177(2008)10-1907-06

* 国家自然科学基金(批准号:50535030,50775209)及新世纪优秀人才支持计划资助项目

[†] 通信作者. Email: tong-zhaomin@sohu.com

2008-01-12 收到, 2008-06-18 定稿